THE JOURNAL OF PHYSICAL CHEMISTRY Letters

pubs.acs.org/JPCL

Adaptive Accelerated Molecular Dynamics (Ad-AMD) Revealing the Molecular Plasticity of P450cam

Phineus R. L. Markwick,*[,†,#,§] Levi C. T. Pierce,[†,§] David B. Goodin,[‡] and J. Andrew McCammon[†,#]

[†]Department of Chemistry and Biochemistry, University of California—San Diego, 9500 Gilman Drive, Urey Hall, La Jolla, California 92003-0365, United States, [‡]Department of Molecular Biology, The Scripps Research Institute, 10550 North Torrey Pines Road, La Jolla, California 92037, United States, and [#]Howard Hughes Medical Institute, 4000 Jones Bridge Road, Chevy Chase, Maryland 20815-8500, United States

ABSTRACT An extended accelerated molecular dynamics (AMD) methodology called adaptive AMD is presented. Adaptive AMD (Ad-AMD) is an efficient and robust conformational space sampling algorithm that is particularly-well suited to proteins with highly structured potential energy surfaces exhibiting complex, large-scale collective conformational transitions. Ad-AMD simulations of substrate-free P450cam reveal that this system exists in equilibrium between a fully and partially open conformational state. The mechanism for substrate binding depends on the size of the ligand. Larger ligands enter the P450cam binding pocket, and the resulting substrate-bound system is trapped in an open conformation via a population shift mechanism. Small ligands, which fully enter the binding pocket, cause an induced-fit mechanism, resulting in the formation of an energetically stable closed conformational state. These results are corroborated by recent experimental studies and potentially provide detailed insight into the functional dynamics and conformational behavior of the entire cytochrome-P450 superfamily.

SECTION Biophysical Chemistry

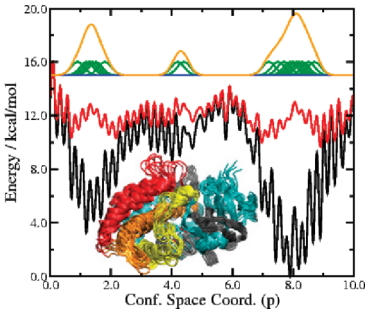

The function of biomacromolecules is determined by both their 3D structure and dynamics.[1,2] Proteins are inherently flexible systems displaying a broad range of dynamics over a hierarchy of time scales. Many biologically important processes, such as enzyme catalysis,[3] ligand binding, and signal transduction,[4] occur on the microsecond—millisecond time scale.[5] The study of such slow time scale dynamics remains a challenge to experimentalists and theoreticians alike. Despite the sustained and rapid increase in available computational power and the development of efficient simulation algorithms, MD simulations of large proteins and biomachines are generally limited to time scales of tens to hundreds of nanoseconds. Considerable progress has been made in the development of more sophisticated methods to sample the conformational space of proteins more efficiently,[6,7] allowing the study of functionally important slow molecular motions. In general, these methods can be divided into two groups. The first involves the identification of transition pathways between known initial and final states. Such methods include transition path sampling[8] and targeted molecular dynamics.[9] The second group contains those methods that efficiently sample low-energy molecular conformations, allowing the rapid identification of thermodynamically dominant regions on the potential energy surface (PES). These methods include replica exchange MD,[10] meta-dynamics,[11] and accelerated molecular dynamics (AMD).[12] The principle behind AMD is to add a continuous non-negative bias potential to the actual PES, which raises the low-energy regions on the potential energy landscape, decreasing the magnitude of the energy barriers and accelerating the exchange between low-energy conformational states while still maintaining the essential details of the underlying potential energy landscape. One of the favorable characteristics of this method is that it yields a canonical average of an observable, so that thermodynamic and other equilibrium properties can be determined.

AMD has already been successfully employed to study slow time scale dynamics in small proteins, such as ubiquitin[13] and IκBα.[14] The enhanced conformational space sampling by AMD in these studies was shown to significantly improve the theoretical prediction of experimental NMR observables, such as residual dipolar couplings,[13,14] scalar J couplings,[13,15] and chemical shifts[16] that are sensitive to dynamic averaging on the micro- to millisecond time scale. As a robust free-energy sampling method, AMD has also been successfully combined with molecular modeling approaches to study the conformational behavior of natively unstructured proteins.[17]

Received Date: October 27, 2010
Accepted Date: January 4, 2011
Published on Web Date: January 07, 2011

DOI: 10.1021/jz101462n | *J. Phys. Chem. Lett.* **2011**, *2*, 158–164

Despite these initial successes, certain aspects of the AMD methodology, including both efficiency and versatility, need to be improved in order to study more complex dynamic behavior in large biomolecular systems. In light of this, we have developed an extended AMD methodology called adaptive AMD (Ad-AMD).

The principal idea behind Ad-AMD is to use the information that is obtained about the potential energy landscape of the system during an AMD simulation to optimize the acceleration parameters in order to sample the conformational space more efficiently. Ostensibly, by learning from the simulation itself, the acceleration parameters are adapted to create an optimal modified "history-dependent" PES. Ad-AMD provides efficient and enhanced conformational sampling for systems exhibiting a highly structured potential energy landscape. History-dependent adaption of the acceleration level during the course of the simulation allows the system to rapidly traverse exceedingly large energy barriers, identifying complex, collective conformational transitions while still maintaining the integrity of the underlying PES. In this paper, we introduce the Ad-AMD method and apply it to the study of the molecular plasticity and functional dynamics of P450cam from *Pseudomonas putida*.

P450cam (CYP101) is a member of the cytochrome-P450 superfamily, a large and diverse group of heme mono-oxygenases that activate O_2 for oxygen insertion into a wide variety of substrates. Previous X-ray crystallographic studies have shown that P450cam can be trapped in a range of conformational states. While camphor-bound P450cam adopts a "closed" conformation,[18,19] a variety of "open" conformations have been observed in response to binding large tethered adamantane probes.[20−22] Substrate-free P450cam has long been regarded to exist in the closed state following the report of a substrate-free structure obtained by soaking dithiothreitol (DTT) out of the active site of crystals, affording a conformation very similar to the camphor-bound form.[23] Small-angle X-ray scattering[24] and hydrostatic pressure[25,26] experiments have also supported the view that substrate-free P450cam exists in a closed conformation. However, these studies have recently been brought into question following the observation of an open conformation of P450cam in the absence of substrate.[27]

The details of accelerated molecular dynamics have been discussed previously in the literature,[12] and we merely provide a brief summary here. In the standard AMD formalism, a continuous non-negative bias potential, $\Delta V(\mathbf{r})$, is defined such that when the true underlying potential of the system, $V(\mathbf{r})$, lies below a certain threshold boost energy, E_b, the simulation is performed on a modified potential, $V^*(\mathbf{r}) = V(\mathbf{r}) + \Delta V(\mathbf{r})$, but when $V(\mathbf{r}) \geq E_b$, the simulation is performed on the true potential [$V^*(\mathbf{r}) = V(\mathbf{r})$]. The modified potential is related to the true potential, bias potential and boost energy by[12]

$$\begin{aligned} V^*(\mathbf{r}) &= V(\mathbf{r}) \qquad V(\mathbf{r}) \geq E_b \\ V^*(\mathbf{r}) &= V(\mathbf{r}) + \Delta V(\mathbf{r}) \qquad V(\mathbf{r}) < E_b \end{aligned} \tag{1}$$

and the bias potential, $\Delta V(\mathbf{r})$ is defined as

$$\Delta V(\mathbf{r}) = \frac{(E_b - V(\mathbf{r}))^2}{\alpha + E_b - V(\mathbf{r})} \tag{2}$$

The application of the bias potential results in a raising and flattening of the potential energy landscape, thereby enhancing the escape rate between low-energy conformational states, and the extent of acceleration is determined by the choice of the acceleration parameters E_b and α. In the standard AMD protocol, the parameters E_b and α are kept constant.

A more efficient extension to the accelerated molecular dynamics approach is Ad-AMD. In this approach, one of the acceleration parameters (α) is held fixed, and the boost potential, E_b, is adapted in a history-dependent fashion during the AMD simulation using the population statistics on the modified potential. In order to achieve this, it is necessary to project the trajectory onto a suitable predefined conformational subspace. In the present application, the P450cam system was projected onto the conformational subspace defined by the two lowest principal components obtained from a PCA analysis performed on a collection of available X-ray crystal structures of P450cam cocrystallized with different substrates. The adaptive boost potential, $E_b(p,q)$, is then given by

$$E_b(p,q) = E_b(0) + \sum_i a \cdot \exp - \left(\frac{(p - \langle p_{i-1} \rangle)^2}{2c^2} + \frac{(q - \langle q_{i-1} \rangle)^2}{2c^2} \right) \tag{3}$$

where p and q are the projected principal components and the index, i, refers to the number of adaptive Gaussians added to the boost potential during the simulation. The simulation is initiated as a standard AMD simulation with a boost energy of $E_b(p,q) = E_b(0)$ (the base-boost potential). After 500 000 MD steps (the equivalent of 500 ps), the trajectory is projected into the principal component space (p,q), and the average PC-projection coordinates ($\langle p_{i-1} \rangle$,$\langle q_{i-1} \rangle$) are calculated. An adaptive 2D-Gaussian boost potential centered at these coordinates is then added to the boost potential, $E_b(p,q)$, and the simulation is performed for another 500 000 MD steps. The resulting 500 000 structures are projected into the principal component space, and the average PC-projection coordinates are used to define the center of the next adaptive 2D-Gaussian boost potential. In this way, the boost potential is adapted every 500 000 MD steps in a history-dependent fashion. The parameters a and c define the magnitude and width of the adaptive Gaussian boost potentials, respectively. In the pres ent work, "dual boost" Ad-AMD simulations were performed, in which two adaptive acceleration potentials were applied to the P450cam system. The first acceleration potential was applied to the torsional potential only, and a second, weaker acceleration was applied across the entire potential. A schematic representation of the Ad-AMD method is shown in Scheme 1.

All MD, AMD, and Ad-AMD simulations presented in this work were performed on a 404 residue construct of substrate-free P450cam using an in-house modified version of the AMBER10 simulation suite.[28] The ff99SB force field[29] was employed for the solute residues (Leu11−Val414), with the exception of a nonstandard Cys357-heme residue for which a force field was generated in-house, and the TIP4P water force field was used for the solvent molecules. A comparative

DOI: 10.1021/jz101462n | J. Phys. Chem. Lett. 2011, 2, 158–164

Scheme 1. Schematic representation of the adaptive AMD method[a]

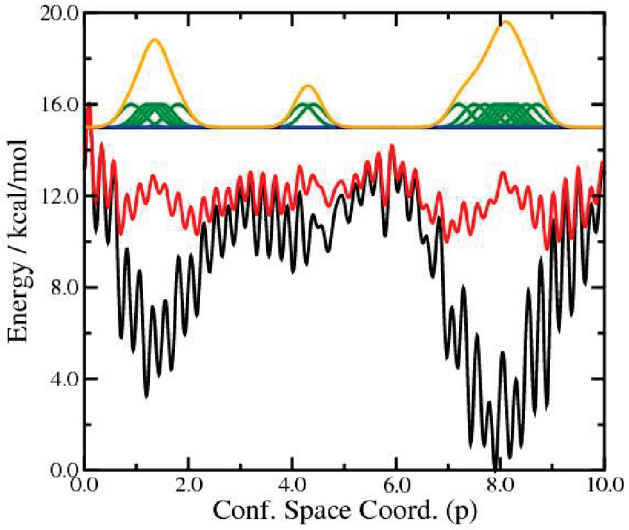

[a] The rugged and highly structured true PES of the protein as a function of the configurational space coordinate, p, is shown in black. The base-boost potential, $E_b(0)$ is fixed at 15 kcal/mol above the potential energy minimum (blue line). The history-dependent adaptive Gaussian boost potentials are shown in green. The final adaptive boost potential, $E_b(p)$, is shown in orange, and the resulting modified potential energy surface on which the system evolves during the Ad-AMD simulation is represented by the red line using the fixed acceleration parameter α = 12 kcal/mol.

analysis of previous dual-boost AMD simulation studies[13,14,30] identified that for torsional acceleration, the optimal value of $[E_b(\text{dih}) - V_0(\text{dih})]$ (where $V_0(\text{dih})$ is the average torsional potential energy obtained from a standard MD simulation) is approximately equal to 3−5 kcal/mol times the number of solute residues, and the associated acceleration parameter, $\alpha(\text{dih})$, is equal to 1/5 of this value. For the background total acceleration, $[E_b(\text{tot})-V_0(\text{tot})]$ and $\alpha(\text{tot})$ should both be equal to 0.16 kcal/mol times the number of atoms in the simulation cell (NASC).[31] In light of this, the acceleration parameters employed for all standard AMD simulations in this work are $\{[E_b(\text{dih})-V_0(\text{dih})], \alpha(\text{dih}); [E_b(\text{tot})-V_0(\text{tot})], \alpha(\text{tot})\} = \{1400, 280; 0.16\text{NASC}, 0.16\text{NASC}\}$ kcal/mol. The acceleration parameters used for all of the Ad-AMD simulations in this work are $\{[E_b(\text{dih})(0) - V_0(\text{dih})], \alpha(\text{dih}); [E_b(\text{tot})(0) - V_0(\text{tot})], \alpha(\text{tot})\} = \{700, 280; 0.08\text{NASC}, 0.16\text{NASC}\}$ kcal/mol. Notice that for both torsional and total acceleration terms, the respective α values are held constant and are the same as those used for the standard AMD simulations. However, in each case, the base-boost potential, $E_b(0)$ has been substantially lowered. The strength of the adaptive Gaussian bias potentials, a, was set to 10.0 kcal/mol for the torsional acceleration and $0.01\text{-}[E_b(\text{tot})(0) - V(\text{tot})]$ for the total background acceleration. The width of the adaptive Gaussian potentials, c = 1.80 Å, was defined such that the full width of the adaptive Gaussian bias potential in the {PC1,PC2} projection space encompassed the entire PC-projection space sampled by a standard 5 ns MD simulation of substrate-free P450cam. The reader is referred to the SI for a discussion of the specific choice of Ad-AMD parameters used, as well as for full simulation details.

The five X-ray crystal structures of P450cam (PDB Ids: 5CP4, 1RE9, 1RF9, 3P6T, 3P6X) projected onto their own principal components {PC1,PC2} are depicted in Figure 1. The closed P450cam-camphor conformation is located at {−25.82,−6.87}, and the most open conformation (P450cam-AdaC3-C8-Dans) is located at {21.01,−5.77}. For each of these X-ray crystal structures, the substrate was removed, and a standard 5 ns classical MD (CMD) simulation was performed. In all five CMD simulations, the system was found to be stable, affording backbone RMSDs to the respective X-ray crystal structure of 1.0−1.2 Å. The results of these initial simulations suggest that P450cam is stable in both closed and open conformations in the absence of the respective substrate. The conformational space sampling of a standard 25 ns CMD simulation for the closed conformation projected onto the principal component space is shown in Figure 1 (black circles).

A 25 000 000 step standard AMD simulation initiated in the closed conformation was performed, and the (unweighted) conformational space sampling is depicted in blue (Figure 1). The AMD trajectory clearly samples more conformational space than the standard CMD simulation, identifying a large number of substates as the system oscillates back and forth about the native closed conformation. However, even under these acceleration conditions, the system never exits the closed state. In comparison, a 25 000 000 step Ad-AMD simulation initiated in the closed state (shown in red in Figure 1) reveals the true molecular plasticity of substrate-free P450cam. In the first half of the Ad-AMD simulation, the system resides broadly in the closed conformation, and a considerable amount of adaptive bias is applied before the system exits the closed state and then rapidly samples a large number of open conformational states. The conformational space sampling observed in the Ad-AMD simulation not only encompasses all five X-ray crystal structures but also identifies new extended open conformations. An ensemble of structures collected over the Ad-AMD simulation is shown in Chart 1.

The Ad-AMD simulation reveals a complex collective motion of substrate-free P450cam involving predominantly the F and G helices and the F−G loop, as well as the H, I, B, and C helices and the B−C loop, which is seen to be considerably more flexible in the open conformational states. As such, over one-third of the residues in the protein are specifically involved in the functional dynamics of the system, a result which is quantitatively represented in Figure 2.

As a robust conformational space sampling protocol, the Ad-AMD approach is obviously much more efficient than standard AMD. Interestingly, the magnitude of the bias potential applied to the system in the Ad-AMD method is considerably lower than that applied during the standard AMD simulation. The enhanced efficiency of Ad-AMD arises from the fact that, rather than raising and flattening the entire PES, the adaptive bias potential is selectively applied only to the lowest-energy regions on the underlying PES. As the perturbation applied to the system is, on average, much smaller, the resulting trajectory affords a much higher level

DOI: 10.1021/jz101462n | J. Phys. Chem. Lett. 2011, 2, 158–164

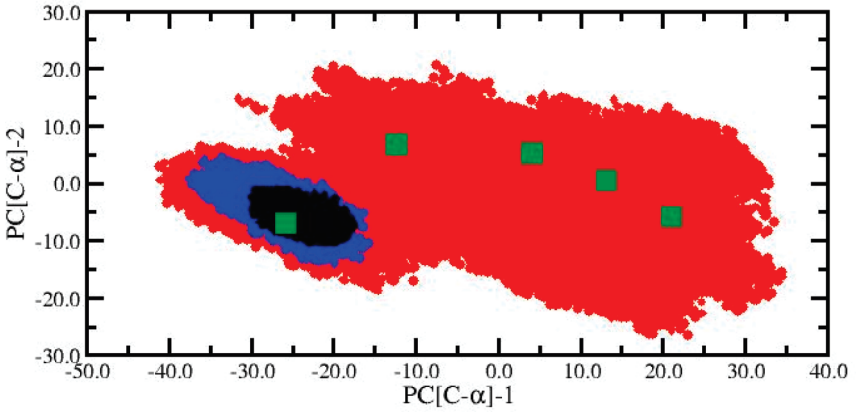

Figure 1. The conformational dynamics of substrate-free P450cam projected into the principal component space {PC1,PC2} obtained from a PCA analysis of five X-ray crystal structures (green squares). The black circles represent the conformational space sampling afforded by a standard 25 ns classical MD simulation. The blue circles represent the conformational space sampling afforded by a standard 25 000 000 step AMD simulation. The red circles represent the conformational space sampling obtained from a 25 000 000 step Ad-AMD simulation. All simulations were initiated in the closed conformation located at {PC1,PC2} = {−25.82,−6.87}.

Chart 1. Ensemble of Structures for Substrate-Free P450cam Extracted from the Ad-AMD Simulation Superposed by Performing a Backbone RMSD Fit to Residues 295−405 (gray)[a]

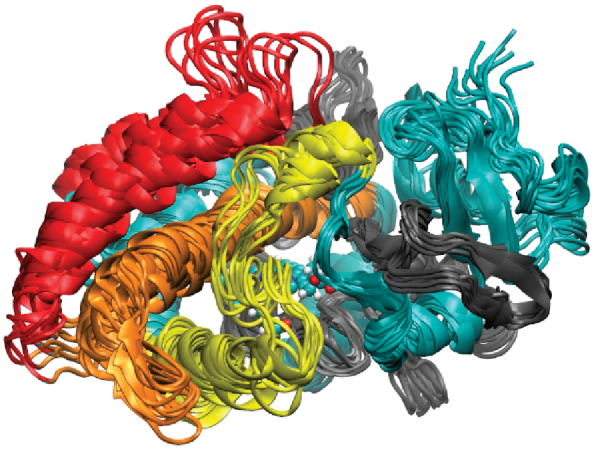

[a] The Ad-AMD simulation reveals a complex collective motion of substrate-free P450cam involving predominantly the F and G helices and the FG loop (red), as well as the H and I helices and the H−I loop (orange) and the B and C helices and the B−C loop (yellow). The remainder of the protein is shown in cyan.

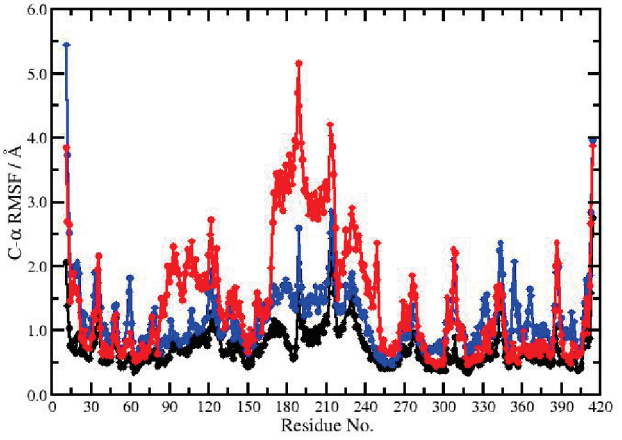

Figure 2. C-α atom root-mean-square fluctuation (RMSF) obtained from the standard 25 ns MD simulation (black), the 25 000 000 step AMD simulation (blue), and the 25 000 000 step Ad-AMD simulation (red) of substrate-free P450cam initiated in the closed state. In each case, the structures collected across the ensemble were first superposed by performing a backbone RMSD fit to residues 295−405. A significant increase in the RMSFs from the Ad-AMD simulation is observed in the B and C helices and the B−C loop (residues 89−120) and the F, G, H, and I helices and the F−G and H−I loops (residues 171−267).

of structural integrity. During the Ad-AMD simulation, the system was seen to come to within 1.3 Å of the backbone RMSD for all five X-ray crystal structures, a remarkable result considering that the backbone RMSD afforded by the CMD simulations initiated in these different conformations was found to be 1.0−1.2 Å.

A qualitative representation of the free-energy surface can be readily obtained from the Ad-AMD simulation by analyzing the magnitude of the adaptive boost energy across the conformational space, as shown in Figure 3.

Obviously the lowest free-energy conformations are associated with those regions where it was necessary to apply the largest adaptive boost potential. We clearly observe three local free-energy minima. The lowest energy state appears to be the closed conformation, broadly located at {PC1,PC2} = {−28.0,−5.0}. In addition, we observe two other local free-energy minima associated with a fully open {18.0,−18.0} and partially open {−14.0,4.0} conformational state. However, the free-energy statistics alone do not provide the complete story. We noticed during the Ad-AMD simulation that once the system had exited the closed state, it rapidly moved between the fully and partially open states but never returned to the closed conformation. This was a surprising result as we expected to see the system freely exchange between the closed and open states on the adaptive modified potential. We subsequently performed four more 25 000 000 step Ad-AMD simulations, this time initiating the simulations in the open conformational states using the atomic coordinates from the available X-ray crystal

DOI: 10.1021/jz101462n | J. Phys. Chem. Lett. 2011, 2, 158–164

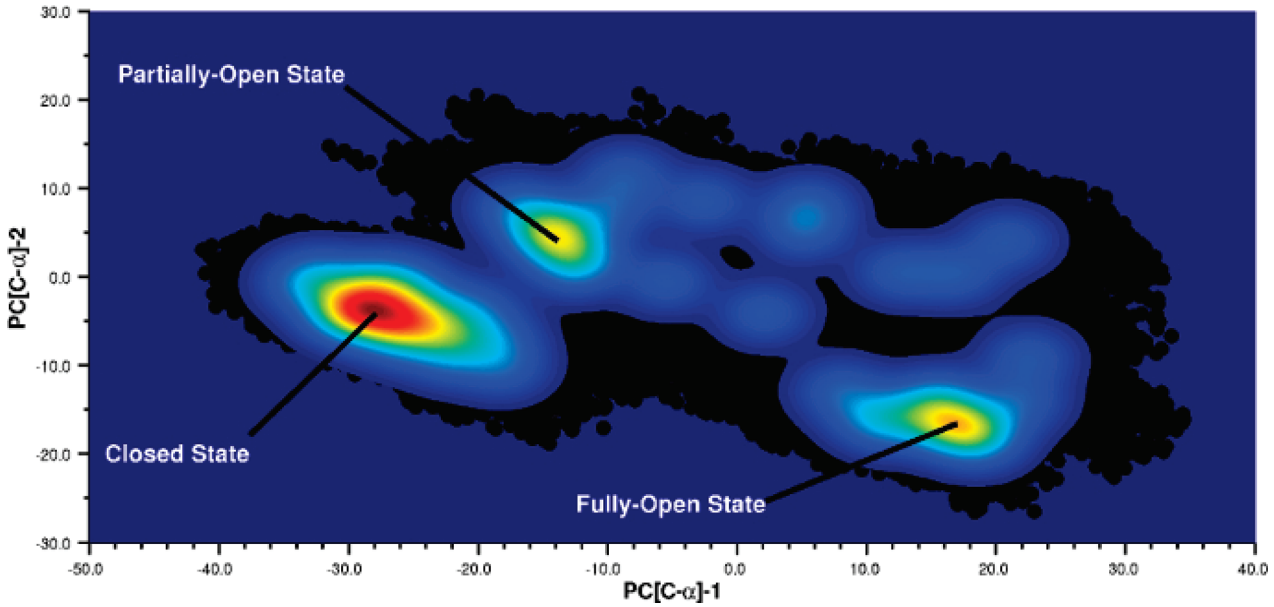

Figure 3. Variation in the adaptive boost potential, $E_b(p,q)$ in the projected principal component space {PC1,PC2} obtained from the Ad-AMD simulation initiated in the closed state. The lowest boost potential (the base-boost potential) is shown in blue, and the largest boost potential, affording the most aggressive acceleration, is shown in red. The black circles represent the conformational space sampling obtained from the 25 000 000 step Ad-AMD simulation.

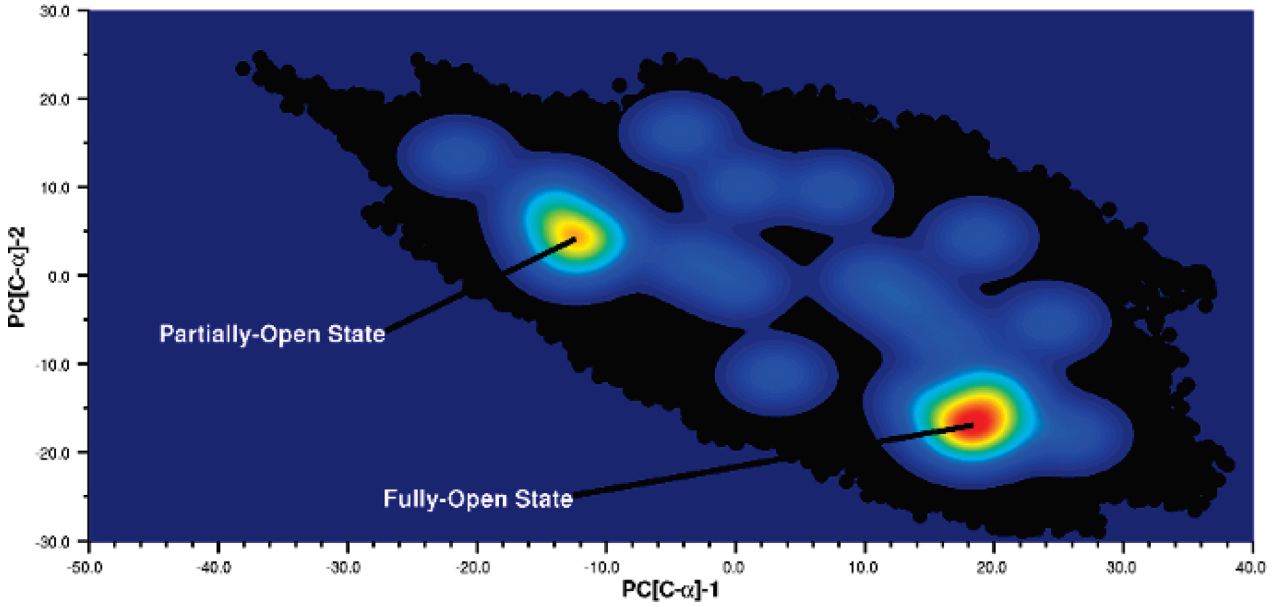

Figure 4. Variation in the adaptive boost potential, $E_b(p,q)$ in the projected principal component space {PC1,PC2} obtained from a representative Ad-AMD simulation of substrate-free P450cam initiated in the open state (using the X-ray crystal structure coordinates from P450cam-AdaC3-C8-Dans). The lowest boost potential (the base-boost potential) is shown in blue, and the largest boost potential, affording the most aggressive acceleration, is shown in red. The black circles represent the conformational space sampling obtained from the 25 000 000 step adaptive AMD simulation. The adaption of the modified potential was terminated after 15 000 000 steps (see text). Notably, in comparison to the conformational space sampling obtained from the Ad-AMD simulation initiated in the closed state (Figures 2 and 3), the closed conformation is never visited during the simulation.

structures. In all four of these Ad-AMD simulations, within 15 000 000 steps, the system sampled the entire open configurational space and exchanged so rapidly between the (already sampled) fully and partially open states that the addition of further adaptive Gaussian boost potentials was no longer appropriate. For the remainder of the simulation, the adaption was therefore switched off. The Ad-AMD simulations readily identified the two local free-energy minima associated with the fully open and partially open conformational states but never visited the closed conformation, as shown in Figure 4.

DOI: 10.1021/jz101462n | J. Phys. Chem. Lett. 2011, 2, 158–164

It should be noted that, unlike several other enhanced conformational space sampling methods in which the system is driven along a predefined reaction coordinate, whether the system would naturally follow that reaction coordinate or not, Ad-AMD will not force a system to undergo an unnatural transition to a kinetically inaccessible state.

The results of all of the Ad-AMD simulations strongly suggest that while the closed conformation is energetically stable, it is kinetically inaccessible to substrate-free P450cam. Therefore, we propose that substrate-free P450cam exists in equilibrium between a fully open and partially open state, located at {PC1,PC2} = {18.0,−18.0} and {−14.0,4.0}, respectively (Figure 4). The lowest-energy, and hence most populated, conformation is the fully open state. As such, P450cam can accommodate a variety of substrates of differing size. Larger ligands can enter the binding pocket when P450cam exists in the fully open state and the resulting substrate-bound system is trapped in an open conformation via a population shift mechanism. However, when a small ligand, such as camphor or DTT, fully enters the binding pocket, it triggers an induced-fit mechanism, resulting in the protein "zipping up" around the bound substrate, leading to the formation of an energetically stable closed conformational state. These results are corroborated by recent experimental studies[27] and potentially provide detailed insight into the functional dynamics and conformational behavior of the entire cytochrome-P450 superfamily. Indeed, several other members of the P450 superfamily, most notably P450 EryK[32] and PikC,[33] have also been shown to coexist in open and closed states in the absence of substrate.

In conclusion, we have presented a novel variant of the accelerated molecular dynamics method called adaptive AMD. Ad-AMD is an extremely efficient and robust conformational space sampling algorithm which also affords a qualitatively accurate description of the free-energy surface. A series of Ad-AMD simulations performed on substrate-free P450cam revealed that this system exists in equilibrium between a fully open and partially open conformational state. The mechanism for substrate binding to P450cam depends on the size of the ligand. Larger ligands enter the P450cam binding pocket, and the resulting substrate-bound system is trapped in an open conformation via a population shift mechanism. Small ligands, such as camphor or DTT, which fully enter the binding pocket, cause an induced-fit mecha nism, resulting in the formation of an energetically stable closed conformational state.

SUPPORTING INFORMATION AVAILABLE Computational details, PCA protocol, discussion of the specific choice of AMD and Ad-AMD parameters, and the relative efficiency of the two methods. This material is available free of charge via the Internet at http://pubs.acs.org.

AUTHOR INFORMATION

Corresponding Author:

*To whom correspondence should be addressed. E-mail: pmarkwick@ucsd.edu.

Author Contributions:

§ These authors contributed equally to this work.

ACKNOWLEDGMENT P.R.L.M. gratefully acknowledges HHMI for financial support. Work at UCSD is supported in part by the NSF, NIH, CTBP, NBCR, and the NSF Supercomputer Centers.

REFERENCES

(1) Frauenfelder, H.; Sligar, S. G.; Wolynes, P. G. The Energy Landscapes and Motions of Proteins. *Science* **1991,** *254*, 1598–1603.

(2) Benkovic, S. J.; Hammes-Schiffer, S. A Perspective on Enzyme Catalysis. *Science* **2003,** *301*, 1196–1202.

(3) Tousignant, A.; Pelletier, J. N. Protein Motions Promote Catalysis. *Chem. Biol.* **2004,** *11*, 1037–1042.

(4) Rousseau, F.; Schymkowitz, J. A Systems Biology Perspective on Protein Structural Dynamics and Signal Transduction. *Curr. Opin. Struct. Biol.* **2005,** *15*, 23–30.

(5) Eisenmesser, E. Z.; Bosco, D. A.; Akke, M.; Kern, D. Enzyme Dynamics During Catalysis. *Science* **2002,** *295*, 1520–1523.

(6) Elber, R. Long-timescale Simulation Methods. *Curr. Opin. Struct. Biol.* **2005,** *15*, 151–156.

(7) Berne, B. J.; Straub, J. E. Novel Methods of Simulating Phase Space in the Simulation of Biological Systems. *Curr. Opin. Struct. Biol.* **1997,** *7*, 181–189.

(8) Bolhuis, P. G.; Chandler, D.; Dellago, C.; Geissler, P. L. Transition Path Sampling: Throwing Ropes Over Rough Mountain Passes, in the Dark. *Annu. Rev. Phys. Chem.* **2002,** *53*, 291–318.

(9) Schlitter, J.; Engels, M.; Kruger, P. J. Targeted Molecular Dynamics: A New Approach for Searching Pathways of Conformational Transitions. *J. Mol. Graph.* **1994,** *12*, 84–89.

(10) Mitsutake, A.; Sugita, Y.; Okamoto, Y. J. Replica-Exchange Multicanonical and Multicanonical Replica-Exchange Monte Carlo Simulations of Peptides. I. Formulation and Benchmark Test. *J. Chem. Phys.* **2003,** *118*, 6664–6675.

(11) Laio, A.; Parrinello, M. Computing Free Energies and Accelerating Rare Events with Metadynamics. In *Computer Simulations in Condensed Matter: From Materials to Chemical Biology*; Ferrario, M., Ciccotti, G., Binder, K., Eds.; Springer Verlag: Berlin, Heidelberg, Germany, 2006; Vol. 1, pp 315−347.

(12) Hamelberg, D.; Mongan, J.; McCammon, J. A. Accelerated Molecular Dynamics: A Promising and Efficient Simulation Method for Biomolecules. *J. Chem. Phys.* **2004,** *120*, 11919–11929.

(13) Markwick, P. R. L.; Bouvignies, G.; Salmon, L.; McCammon, J. A.; Nilges, M.; Blackledge, M. Toward a Unified Representation of Protein Structural Dynamics in Solution. *J. Am. Chem. Soc.* **2009,** *131*, 16968–16975.

(14) Cervantes, C. F.; Markwick, P. R. L.; Sue, S. C.; McCammon, J. A.; Dyson, H. J.; Komives, E. A. Functional Dynamics of the Folded Ankyrin Repeats of IκBα Revealed by Nuclear Magnetic Resonance. *Biochemistry* **2009,** *48*, 8023.

(15) Markwick, P. R. L.; Showalter, S. A.; Bouvignies, G.; Bruschweiler, R.; Blackledge, M. Structural Dynamics of Protein Backbone φ Angles: Extended Molecular Dynamics Simulations Versus Experimental ^3J Scalar Couplings. *J. Biomol. NMR* **2009,** *45*, 17–21.

(16) Markwick, P. R. L.; Cervantes, C. F.; Abel, B. L.; Komives, E. A.; Blackledge, M.; McCammon, J. A. Enhanced Conformational Space Sampling Improves the Prediction of Chemical Shifts in Proteins. *J. Am. Chem. Soc.* **2010,** *132*, 1220–1221.

(17) Mukrasch, M. D.; Markwick, P. R. L.; Biernat, J.; Bergen, M.; Bernado, P.; Griesinger, C.; Mandelkow, E.; Zweckstetter, M.; Blackledge, M. Highly Populated Turn Conformations in Natively Unfolded Tau Protein Identified from Residual

Dipolar Couplings and Molecular Simulation. *J. Am. Chem. Soc.* **2007,** *129*, 5235–5243.
(18) Poulos, T. L.; Finzel, B. C.; Gunsalus, I. C.; Wagner, G. C.; Kraut, J. The 2.6-Å Crystal Structure of *Pseudomonas Putida* Cytochrome P-450. *J. Biol. Chem.* **1985,** *260*, 16122–16130.
(19) Poulos, T. L.; Finzel, B. C.; Howard, A. J. High-Resolution Crystal Structure of Cytochrome P450cam. *J. Mol. Biol.* **1987,** *195*, 687–700.
(20) Dmochowski, I. J.; Crane, B. R.; Wilker, J. J.; Winkler, J. R.; Gray, H. B. Optical Detection of Cytochrome P450 by Sensitizer-Linked Substrates. *Proc. Natl. Acad. Sci. U.S.A.* **1999,** *96*, 12987–12990.
(21) Dunn, A. R.; Dmochowski, I. J.; Bilwes, A. M.; Gray, H. B.; Crane, B. R. Probing the Open State of Cytochrome P450cam with Ruthenium-Linker Substrates. *Proc. Natl. Acad. Sci. U.S. A.* **2001,** *98*, 12420–12425.
(22) Hays, A. M. A.; Dunn, A. R.; Chiu, R.; Gray, H. B.; Stout, C. D.; Goodin, D. B. Conformational States of Cytochrome P450cam Revealed by Trapping of Synthetic Molecular Wires. *J. Mol. Biol.* **2004,** *344*, 455–469.
(23) Poulos, T. L.; Finzel, B. C.; Howard, A. J. Crystal Structure of Substrate-Free *Pseudomonas Putida* Cytochrome P-450. *Biochemistry* **1986,** *25*, 5314–5322.
(24) Lewis, B. A.; Sligar, S. G. Structural Studies of Cytochrome P-450 Using Small Angle X-Ray Scattering. *J. Biol. Chem.* **1983,** *258*, 3599–3601.
(25) Di Primo, C.; Deprez, E.; Hoa, G. H.; Douzou, P. Antagonistic Effects of Hydrostatic Pressure and Osmotic Pressure on Cytochrome P-450cam Spin Transition. *Biophys. J.* **1995,** *68*, 2056–2061.
(26) Fischer, M. T.; Scarlata, S. F.; Sligar, S. G. High-Pressure Investigations of Cytochrome P-450 Spin and Substrate Binding Equilibria. *Arch. Biochem. Biophys.* **1985,** *240*, 456–463.
(27) Y-T. Lee, Y.-T.; R.F. Wilson, R. F.; Rupniewski, I.; Goodin, D. B. P450cam Visits an Open Conformation in the Absence of Substrate. *Biochemistry* **2010,** *49*, 3412–3419.
(28) Case, D. A.; Darden, T. A.; Cheatham, T. E.; Simmerling, C. L.; Wang, J.; Duke, R. E.; Luo, R.; Crowley, M.; Ross, W. C.; et al. *AMBER10*; University of California: San Francisco, CA, 2008.
(29) Hornak, V.; Abel, R.; Okur, A.; Strockbine, B.; Roitberg, A.; Simmerling, C. Comparison of Multiple Amber Force Fields and Development of Improved Protein Backbone Param eters. *Proteins: Struct., Funct., Bioinf.* **2006,** *65*, 712–725.
(30) Grant, B. J.; Gorfe, A. A.; McCammon, J. A. Ras Conformational Switching: Simulating Nucleotide Dependent Conformational Transitions with Accelerated Molecular Dynamics. *PLOS Comput. Biol.* **2009,** *5*, e1000325.
(31) Hamelberg, D.; de Oliveira, C. A. F.; McCammon, J. A. Sampling of Slow Diffusive Conformational Transitions with Accelerated Molecular Dynamics. *J. Chem. Phys.* **2007,** *127*, 155102.
(32) Savino, C.; Montemiglio, L. C.; Sciara, G.; Miele, A. E.; Kendrew, S. G.; Jemth, P.; Gianni, S.; Vallone, B. Investigating the Structural Plasticity of a Cytochrome P450: Three Dimensional Structures of P450 EryK and Binding to its Physiological Substrate. *J. Biol. Chem.* **2009,** *284*, 29170–29179.
(33) Sherman, D. H.; Li, S.; Yermalitskaya, L. V.; Kim, Y.; Smith, J. A.; Waterman, M. R.; Podust, L. M. The Structural Basis for Substrate Anchoring, Active Site Selectivity and Product Formation by P450 PikC from *Streptomyces Venezuelae*. *J. Biol. Chem.* **2006,** *281*, 26289–26297.

DOI: 10.1021/jz101462n | *J. Phys. Chem. Lett.* **2011,** *2*, 158–164